Journal of Scientific Exploration. Vol. 5, No. 1, pp. 121–144, 1991
Pergamon Press plc. Printed in the USA.

0892–3310191 $3.00+.00

Low-Frequency Seismogenic Electromagnetic Emissions as Precursors to Earthquakes and Volcanic Eruptions in Japan

TAKEO YOSHINO

University of Electro-Communications, 1-5-1 Chofugaoka, Chofu-shi, Tokyo 182, Japan

Abstract—A multipoint network was constructed in the Tokyo area for earthquake prediction using seismogenic electromagnetic emissions. The network consists of eight observation points within 50 km of each other. Each point has a digital direction-finding detector with two loop sensors tuned to 82 kHz. The output signals of the receivers are added into a digital vector composition circuit to obtain the direction angle of the source point, and this signal is telemetered to the central computer.

To protect from false alarms caused by local man-made noise interference, the warning is announced only when there is a high cross-correlation between almost all detectors pointing to one small area. The mechanism of these earthquake precursors can be explained as electromagnetic emissions from the rocks around the focus when they are crushed completely by the distortion pressure. These emissions propagate along the fault plane as an EM surface wave mode and radiate from the slit antenna formed by the intersection of the fault plane and ground surface.

In the last five years, we have detected impulsive noise bursts of seismogenic emissions at 82 kHz, 1.525 kHz, and 36 Hz using our multipoint detection network around the Tokyo region and Izu peninsula. This system has recorded EM signals prior to the following events: volcanic eruptions on November 15 and 21, 1986 at Mt. Mihara on Ohshima Island, and on July 12, 1989 in Itoh Bay in the Izu peninsula region, and also a minor earthquake on October 14, 1989 at Ohshima Island.

Introduction

The Japanese–Soviet cooperative project for the study of electromagnetic emission phenomena related to earthquakes was started in 1980. The first emissions were observed at 16:33 JST (UT + 9 hours) on March 31, 1980, at Sugadaira Space Radio Observatory, University of Electro-Communications, Sugadaira, Nagano prefecture in Japan. The magnitude of this earthquake was about 7, and the depth of focus was approximately 380 km. The epicenter was located in the Kyoto prefecture and the distance between the Sugadaira observatory and the epicenter was approximately 250 km. The noise level recorder for 81 kHz registered an anomalously high change in the background noise level, more than 15 dB over the usual level, beginning 50 minutes before the main shock. The noise dropped sharply back to the previous level exactly at the moment of the earthquake as shown in Figure 1. The VLF whistler recorder at Sugadaira Observatory also showed unusual

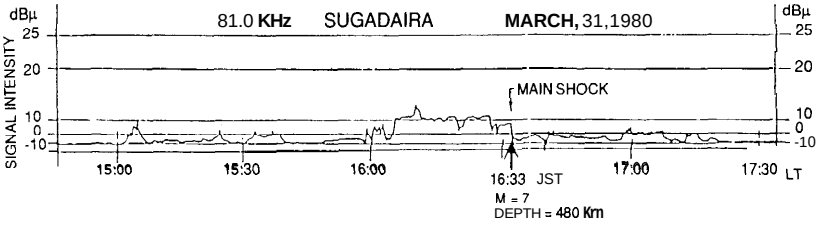

Fig. 1. Electromagnetic radiation level at a frequency of 81 kHz at 16:33 JST (07:33 UT) on March 31, 1980 observed at Sugadaira Space Radio Observatory. (After Gokhberg et al. 1986b.)

impulsive emissions at frequencies below 1.5 kHz before the earthquake as shown in Figure 2. Similar 81–82 kHz emissions were observed prior to other earthquakes of magnitudes 5.5 to 6.5 on September 25, 1980, as shown in Figure 3. These earthquakes were located in the Tokyo suburbs (Gokhberg et al., 1982).

Since 1981, the author and colleagues have observed several emission events in the 81–82 kHz range, just prior to earthquakes. Based on these measurements, we set up a new multipoint observation network with direction finding capabilities around the Tokyo area. The purpose of this network was to investigate the possibility of immediate warning just prior to earthquakes, and elimination of man-made noise interference to improve the accuracy of any potential prediction. One of our most promising results was in the case of an "under foot" earthquake which occurred in southwestern

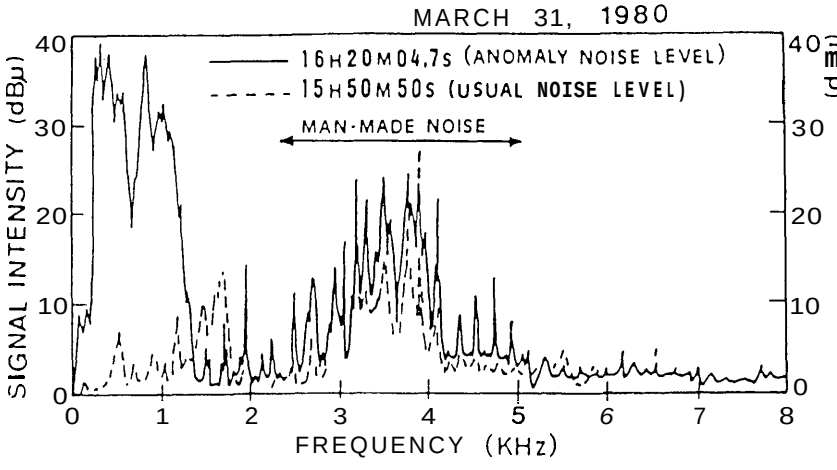

Fig. 2. Spectral amplitude of the sonagram of wide band VLF whistler detector in Sugadaira observatory at 16:20:04.7 JST (about 13 minutes before the earthquake) for the highest noise level of the wave packets and also at 15:50:50 JST (17 minutes after the earthquake) as an example of the usual noise level. (After Gokhberg et al. 1986b.)

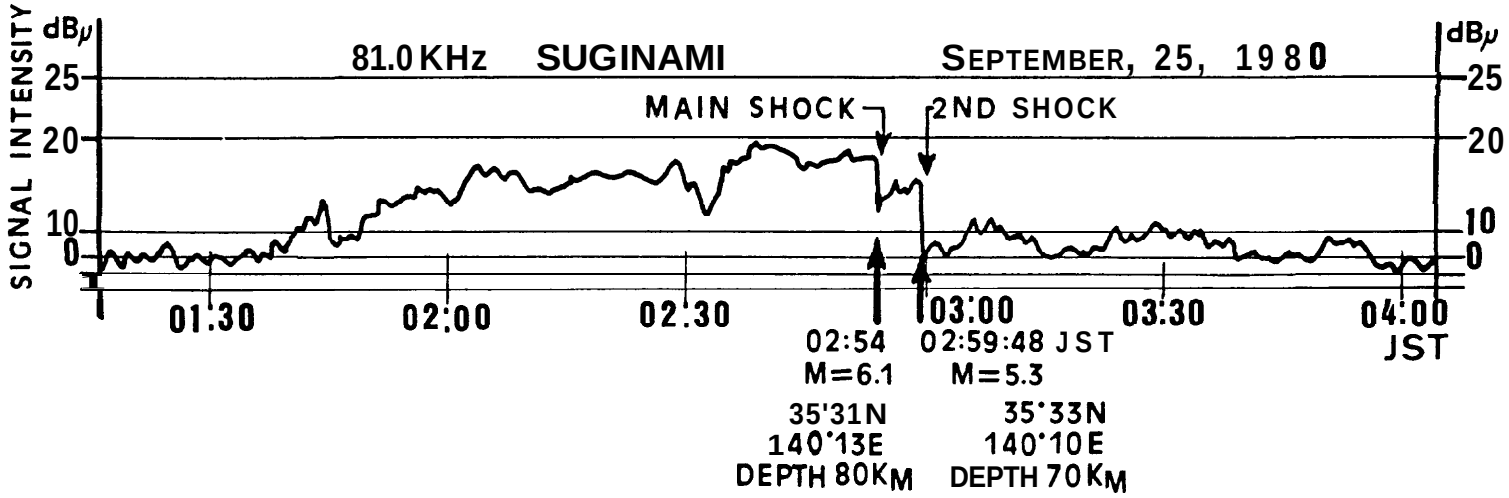

Fig. 3. Electromagnetic radiation level at 81 kHz, 02:54 JST, September 25, 1980, observed at Suginami in the western suburbs of Tokyo. (After Gokhberg et al. 1986b.)

Ibaragi prefecture at 21:14 JST on February 27, 1982. The magnitude of this earthquake was 6.3 and the depth of focus was approximately 40 km, as shown in Figure 4a and b. This retrospective prediction of the epicenter was the result of direction finding from the following three observation points: Suginami in Tokyo, Sugito in Saitama prefecture, and Yatsugatake in Nagano prefecture. The earthquake subsequently occurred in the predicted area, as shown in Figure 4c (Yoshino et al., 1985).

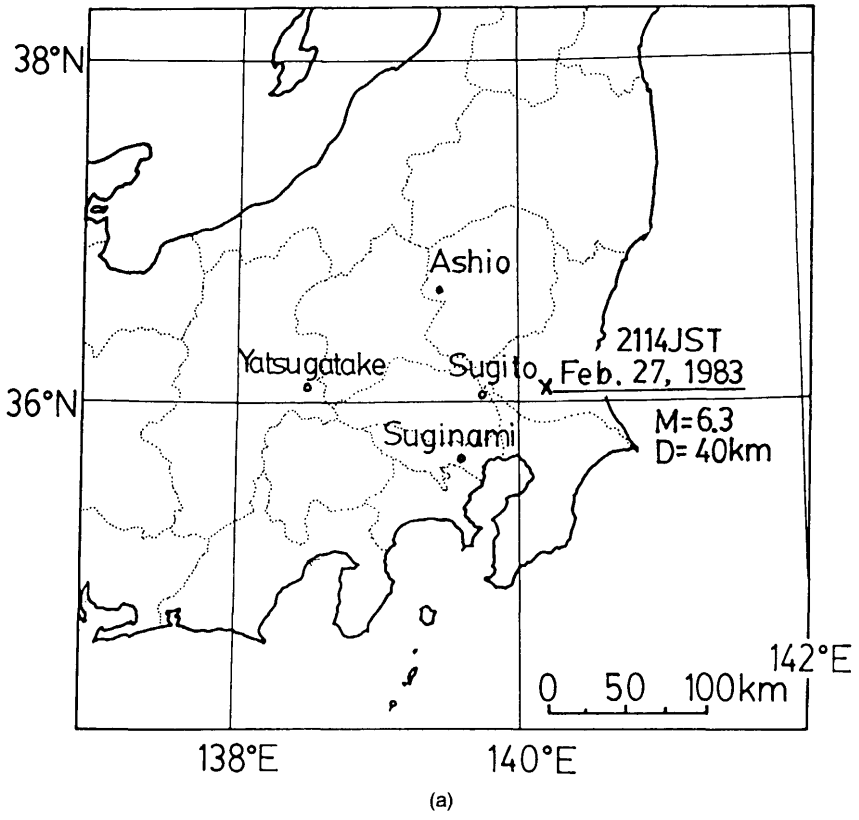

Fig. 4. (a) Locations of observation points and epicenter of the earthquake at 21:14 JST on February 27, 1983. (b) Levels of emissions at Sugito, Suginami, and Yatsugatake observation points before the earthquake. The traces from top to bottom illustrate the variation in signal level for the north–south direction at Sugito, and the east–west and north–south directions at Suginami and Yatsugatake. East–West data from Sugito are missing owing to preamplifier failure. A great number of anomalous emissions with short duration appeared between 12:30 and 21:30 JST at Sugito and Suginami. Anomalies at Yatsugatake appeared after local sunset (19:10). These emissions were recorded independently at each point, but a number of occurrence times show good coincidence with each other. (c) Intersection of the bearings of the anomalous electromagnetic emissions. These bearings are calculated from the data of Suginami at 19:14 and 20:09 JST, and of Yatsugatake at 20:00 and 20:09 JST. The ruled area shows the epicenter area predicted by the emission data. "×" indicates the actual epicenter which falls within the predicted area. (After Yoshiro et al. 1985.)

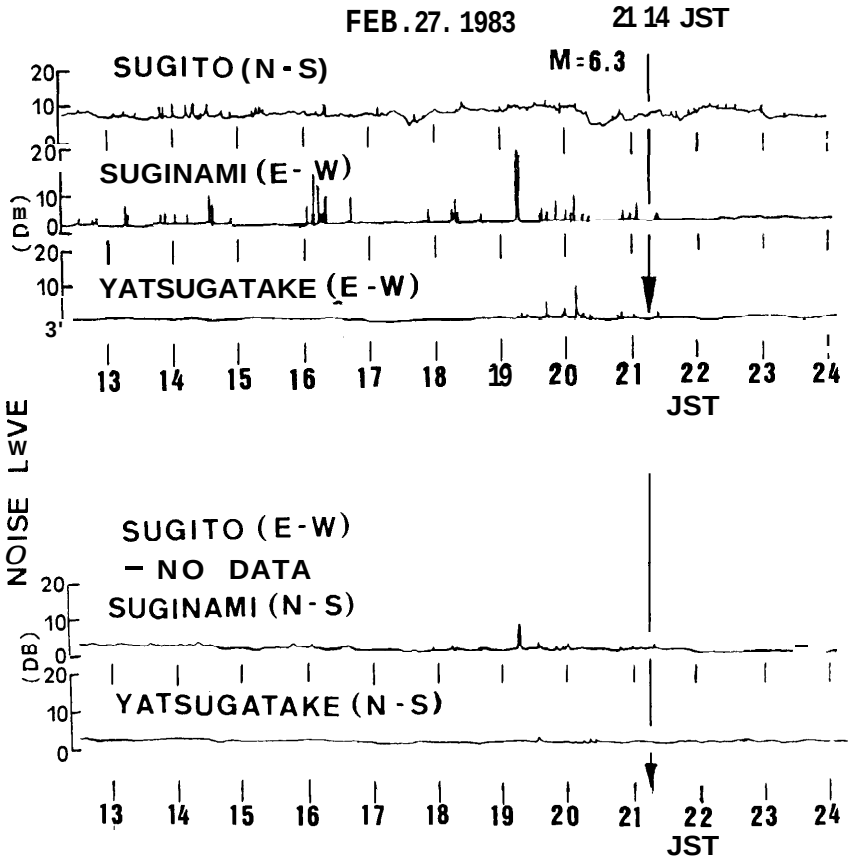

(b)

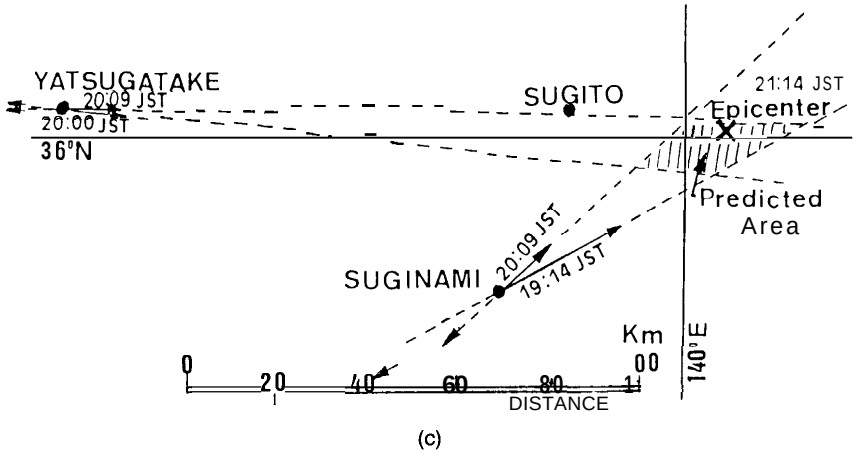

(c)

Fig. 4. *(continued)*

Since 1984, the authors have set up a multipoint direction finding network with eight observation points around the Tokyo region. The locations of observation points are shown in Figure 5. Now, we are building a data telemetry system for realtime cross-correlations (Yoshino, 1986a, 1986b).

A major volcanic eruption occurred on Mt. Mihara in November 1986, and the 82 kHz direction-finding network operating on Ohshima Island recorded several impulsive noise emissions prior to eruptions. Since 1987, we have added two frequency bands [VLF (1.525 kHz) and ELF (36 Hz)] to our multipoint network to improve S/N ratios, owing to increasing 82-kHz background noise levels in the last decade.

In July 1989, the area around the city of Izu Itoh was struck by a series of locally very strong volcanic earthquakes. Izu Itoh is one of the major cities located on the east coast of the Izu peninsula, and the area is famous for its beautiful volcanic mountains, lakes, seaside landscape, and many hot springs. The city extends along the coast of Ito bay, and is located about 35 km northeast of Izu–Ohshima island. These volcanic earthquakes ended with the eruption from a new volcanic crater on the bottom of Ito bay on

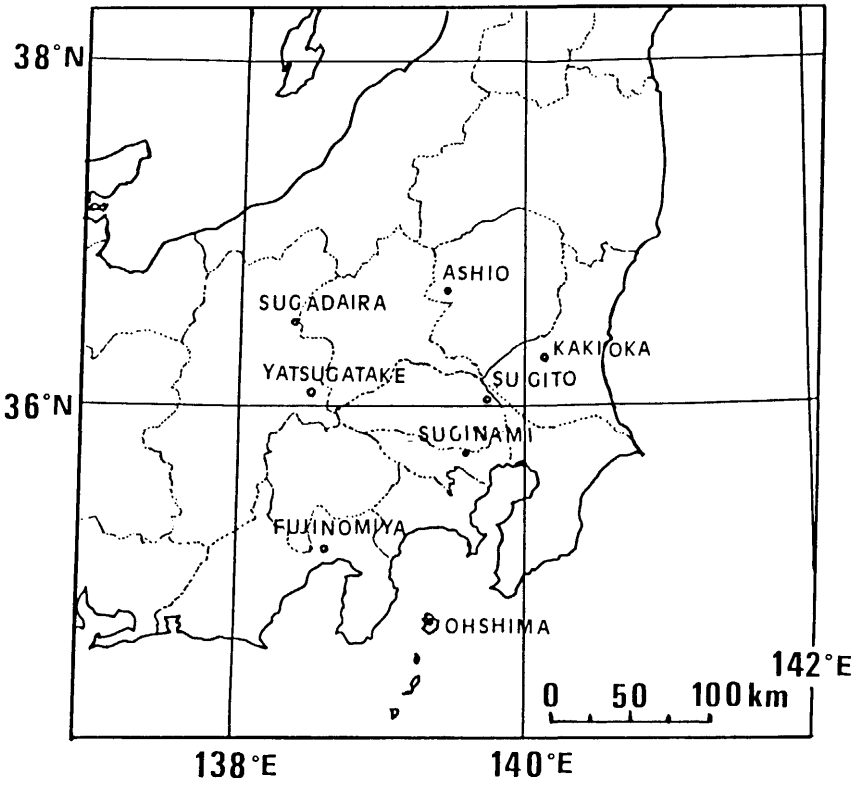

Fig. 5. Location of observation points around the Kanto area as of January 1988.

July 12, 1989. The author obtained several interesting correlations between LF, VLF, and ELF emissions related to these earthquakes.

Radiation Mechanisms

The study of the radiation mechanism of precursory electromagnetic emissions in Japan and the USSR has been ongoing since 1981, but these studies have not obtained any clear and reasonable result until today. Gokhberg and his colleagues in the USSR had tried two different approaches. In the first, they assumed that the source was located in the lower region of the ionosphere and precipitated the plasma instabilities by large gradients of the electric field at the ground surface, dE/dh, and the geomagnetic field intensity at the epicenter region (Gokhberg et al., 1984). In the second, they changed this explanation to electromagnetic emission produced by microdislocations in rocks before shallow earthquakes (Gokhberg et al., 1987). The observation systems and the research approach of the Soviet groups shifted toward lower frequency regions, on the order of a few hertz, because these frequencies were observed in the electric field variations in the lower and upper ionosphere by satellite observations since 1985 (Chmyrev et al., 1987; Larkina et al., 1987; Migulin et al., 1987). We have great trust in these estimations, but the results are not sufficient to explain the source mechanism of the emissions, the mechanism of the electromagnetic energy transmission in the soils and rocks from the earthquake focus to the earth surface, or the mechanism of electromagnetic wave radiation at the surface of the ground.

Laboratory experiments performed by our colleagues show that the rocks emit electromagnetic radiation when crushed (Mizutani & Yamada, 1987). Similar emissions were observed by Cress et al. (1987) in laboratory experiments and by the author in the eruption of Mt. Mihara on November 21, 1986 (Yoshino & Tomizawa, 1989). During the entire duration of the eruption, the emissions were only observed when the dike of magma intruding into the mountain body caused the crushing of rocks.

To explain the mechanism of transmission of electromagnetic impulses from the source around the focus area to the surface of the ground, we have applied a surface mode transmission model. The conductivity along the fault plane is usually very high compared to values in undisturbed rock, and the conductivity gradient is distributed along the direction of fault lines. Such characteristics of a fault surface promote surface mode propagation along the fault plane from the focus to the ground surface. We estimate that the optimum condition for wave propagation is 25 dB/10 km below the usual case for homogeneous soils and rocks at the same distance. To explain the radiation condition at the ground surface, we used the optimum impedance match between the surface and free space and calculated a VSWR of 1.5 using the optimum case when the fault terminates in a slot dipole antenna at the ground surface. Based on these results, the author will attempt to explain

the source mechanisms for the electromagnetic precursor emission phenomena in this article.

Observation Frequencies

Based on very careful searching through the frequency spectrum for several months, the author selected 81–82 kHZ for observation frequencies for seismogenic emissions during the first measurements in 1980, because this range was the only one sufficiently protected from man-made noise sources. This is because so many radio transmitters and other man-made noise sources are widely spread across the frequency spectrum from ELF to EHF on the Japanese islands. Unfortunately, the natural background noise level during the night time at these frequencies of 81–82 kHz is usually 6–10 dB higher than in the daytime, owing to noise signals generated by lightning discharges from tropical thunderstorms. The threshold level of background man-made noise in this frequency range has also been increasing in the last decade. Therefore, the author tried to search for new observation frequency ranges with lower background noise interference. The result was the selection of 1.525 kHz and 36 Hz. The ionospheric propagation of VLF waves is usually a guided mode, and this propagation has a lower cutoff frequency with respect to the dominant frequency. The usual cutoff of dominant modes of the night time ionosphere is approximately 1.8 kHz. Thus, 1.525-kHz waves will not be able to propagate the noise of lightning discharges from the distant tropical regions to middle latitudes. On the other hand, the frequency range from approximately 7–45 Hz is globally very noisy due to the Schumann resonance phenomena. However, the noise spectrum in the Schumann resonance band has characteristics similar to a Gaussian distribution, so the background noise level at 36 Hz will be reduced to a nearly neglegible level. The frequency range below 5 Hz is disturbed by the strong continuous pulsations (PC-1) and (PI-1) emission, and it will be very difficult to clearly select natural noise emission or geomagnetic field pulsation phenomena when observations are made in this frequency range.

Equipment for Detection of Seismogenic Emission

Figure 6 is a block diagram of the new standard detection unit with three frequencies for our multipoint network system, showing the flow of the data processing for the prediction of epicenter bearings by means of electromagnetic precursor emissions at each observation point. As shown in this figure, a sensor for 82 kHz consists of two tuned loop antennas set up perpendicular to one another, north–south and east–west, for direction-finding purposes. Each antenna consists of an 85-cm diameter, 50-turn coil with electrostatic shielding, and tuned to 82 kHz. The two sensors at 1.525 kHz and 36 Hz, added to better exclude man-made noise, consist of 5,000-turn coils with single Permalloy cores 1-cm square by 80-cm long. The output signals from

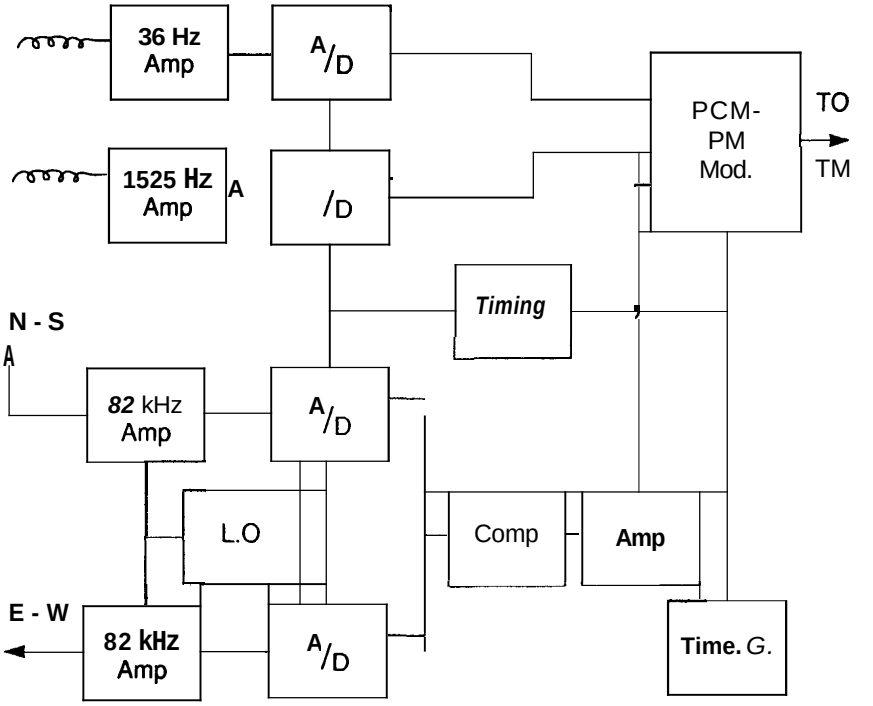

Fig. 6. Block diagram of the data analysis system for electromagnetic earthquake precursor observations.

these coils are transmitted through digital telemetry links to the computer of the earthquake prediction and warning center by telephone cables, microwave links, and optical fiber cables. Data are also stored on digital tape at each observation point. Our test network around the Tokyo area now consists of eight points separated by approximately 50 km.

Protection From Man-Made Noise Interference

The data observed by all observation points are telemetered to the local earthquake prediction and warning center, and are processed to obtain the bearing and location of the noise emission source. To prevent false alarms, we intend to issue an earthquake prediction only when all the computational results of emission bearings are pointed to a single small area with a high level of cross-correlation of most of the bearing data. If a strong noise signal has been received at one observation point, but the computational results of the cross-correlations between almost all other stations do not intersect in a small area, the alarm signal would not be announced. This technique elimi-

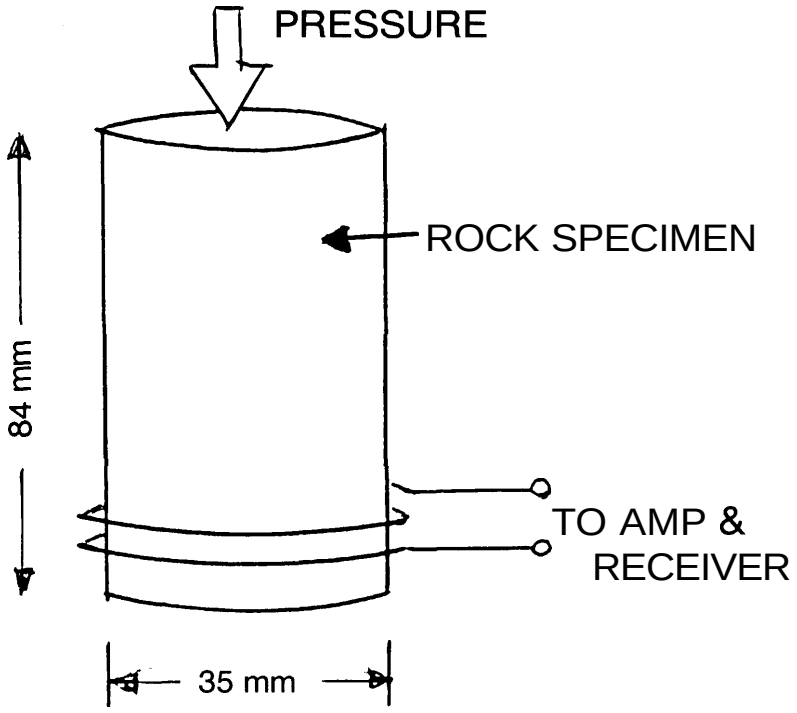

Fig. 7. Size of rock specimen for electromagnetic emission observation, before being crushed by pressure machines (after Mizutani, 1987).

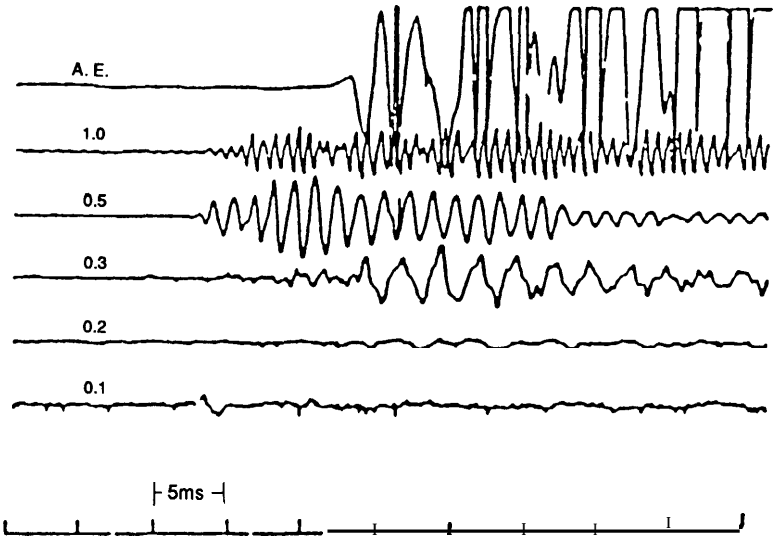

Fig. 8. Acoustic emission (AE) (top) and EM emission wave form observed at 1.0, 0.5, 0.3, 0.2, and 0.1 MHz (second from top to bottom). The time difference between the AE and EM onset times correspond to the travel time of AE (after Mizutani, 1987).

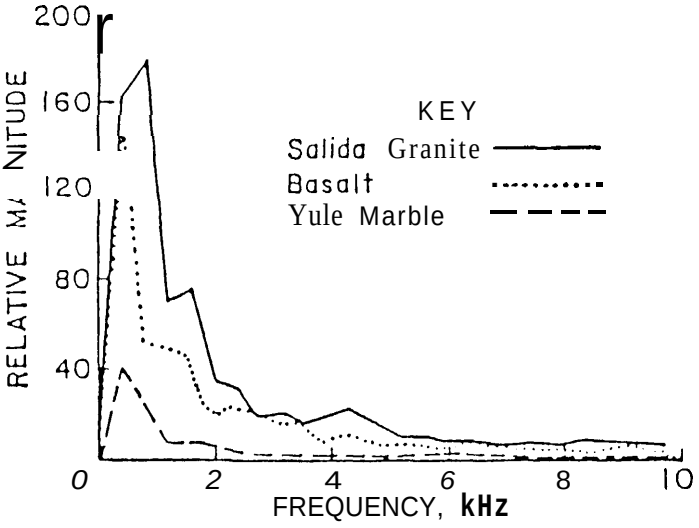

Fig. 9. Laboratory experimental results showing frequency characteristics of emissions when the rock is crushed by a pressure machine (after Cress et al., 1987).

nates man-made noise interference because it is not usually radiated beyond 50 km from its sources.

Model of Radiation Mechanism of Seismogenic Emissions

The author has offered a possible mechanism for the seismogenic electromagnetic radiation above. The emission will be induced as one of the kinds of boundary-charge phenomena when the rocks around the focus of an earthquake are crushed under the very strong distortion forces increasing rapidly just prior to the earthquake. Laboratory experiments have been done by Mizutani and Yamada (1987) and Cress et al. (1987). In these experiments, very strong electromagnetic impulses were observed at the instant the specimen of rock was crushed under high pressure. The values of induced electromagnetic emission obtained were different for each kind of rock, wet or dry, and are dependent on the many different conditions at the time of observations. The size of specimen is shown in Figure 7, and one of the examples of experimental curves is shown in Figure 8. The observation results of Cress et al. are given in Figure 9. Compared with the example of natural emissions observed at Sugadaira, which was shown in Figure 2, the traces of natural and experimental data show very good agreement in frequency characteristics with peaks around 1.5 kHz.

The authors have built a model to explain the radiation mechanisms of seismogenic emission, as shown in Figure 10. Usually the earthquake focus is located on the fault plane as shown in this figure. If the distortion forces are

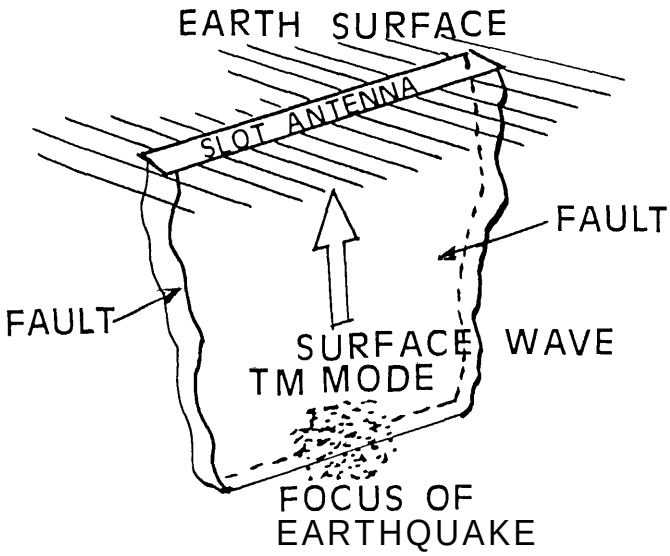

Fig. 10. Model to explain the radiation mechanism of seismogenic emissions.

increased in the fault area, the crushing of pieces of rock is initiated, and the energy of induced electromagnetic impulses is emitted within this region in the fault.

The electrical conductivity inside and directed toward the fault line is usually higher than for the rock outside, this difference being over approximately 20 dB. Also, a sheath structure of high dielectric soils (fault gouge) is often observed on the boundary surface of faults. This condition will be able to support the surface mode of the TEM-electromagnetic wave propagation along the boundary of the fault, and the energy of seismogenic emission will be able to be transmitted from the source depth to the earth's surface with very little attenuation, as compared to the usual plane wave propagation outside the boundary.

The surface mode propagation of electromagnetic waves was developed by Goubou (1950) and Cullen (1954), and today this advanced technique is often applied to microcircuit designs for compact equipment systems in the centimeter- and millimeter-wave bands. The profile of the surface boundary structure is illustrated in Figure 11. As shown in this figure, the boundary surface of a fault has a structure similar to a surface wave transmission line.

The results of the numerical simulation on the estimation of attenuation values for the surface mode wave propagation along the boundary surface of the fault are as follows:

1. resistivity outside of the fault is 10 kΩ/m;
2. resistivity inside of and parallel to the direction of the fault is less than 10 Ω/m;

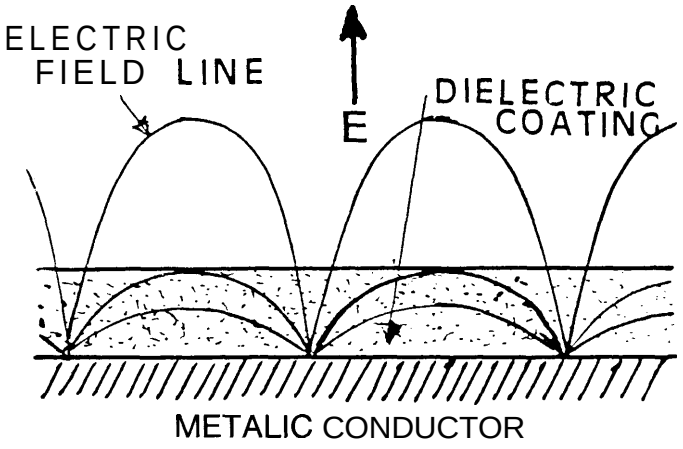

Fig. 11. Structure of a surface wave transmission line and electric field lines of force for the dominant TM mode.

3. specific dielectric constant at the boundary surface of the fault is 20, and outside the area of the fault is 6.0;
4. frequency is 82 kHz, 1.525 kHz, and 36 Hz;
5. depth of focus is 50 km; and
6. TM mode.

The calculated value of total propagation loss when the depth of focus is 50 km for 82 kHz is approximately 63 dB, for the case of dielectric sheath thickness of 10 m, and 65 dB for 20 m. In the case of 1.525 kHz, it is approximately 56 dB in power ratio. If a large quantity of acid water is contained in the fault, the propagation loss will decrease more than 10 dB from the above calculated values. If the ground surface is covered by homogeneous soil and rocks, the value of transmission loss for surface mode propagation is more than 25 dB below the value of plane wave propagation at the same depth.

The radiation impedance matching between surface mode feed and free space radiation mode by a slot antenna, which consists of the boundary between the top end of the fault and the ground surface, was also simulated for many types of matching systems. One of the best cases of VSWR values that can be obtained is 1.5 for the structure shown in Figure 12. We are continuing estimates and experiments on surface mode propagation and impedance-matching for surface radiation by means of a scale model for higher frequencies.

Observation Results at the Eruption of Mt. Mihara

Before July 1986, the volcanic activity at Mt. Mihara had been quiet for the previous 12 years (Weather Record, 1987a). Our observation equipment

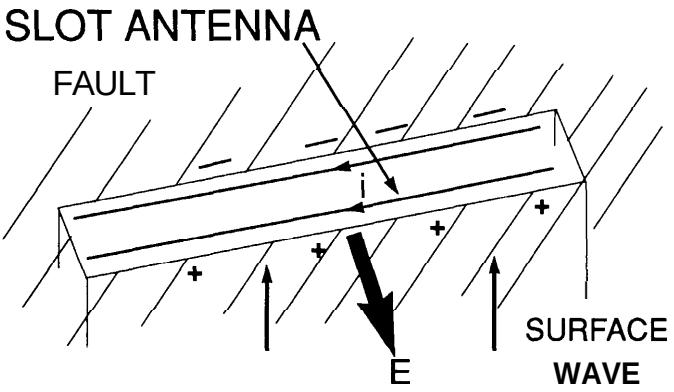

Fig. 12. Structure of a slot antenna on the surface of the ground and a fault excited by a TM mode surface wave.

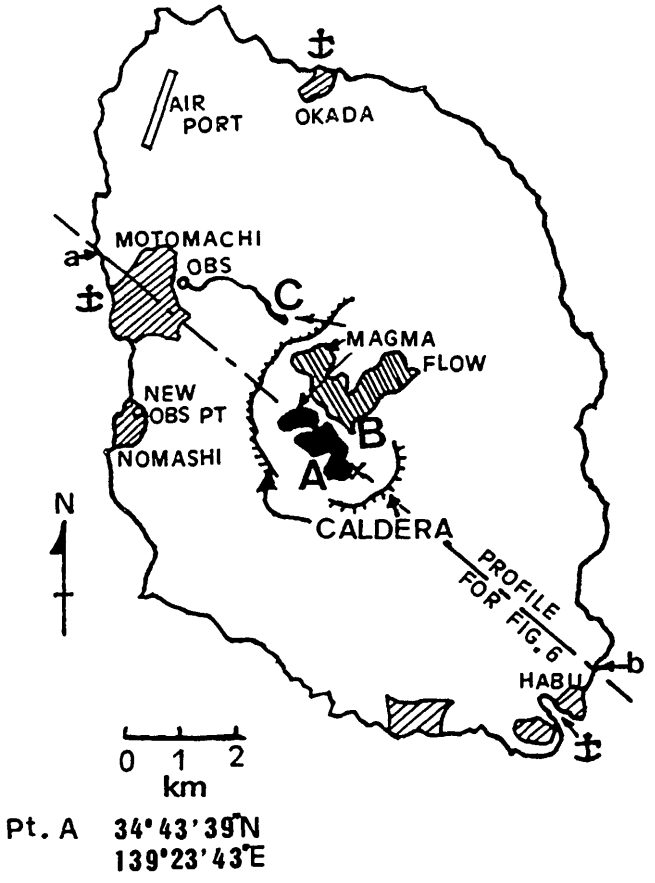

Fig. 13. Map of Izu-Ohshima which illustrates the location of the main eruption, the new craters, and the recording stations. (After Yoshiro et al. 1989.)

was set up in the Ohshima Volcano Observatory of Tokyo University, east of Motomachi, as shown in Figure 13. A typical example of our usual monthly noise conditions data at 82 kHz, recorded by the equipment mentioned above and located at Ohshima, is illustrated in Figure 14a and b. Figure 14a shows the north–south data, Figure 14b the east–west data, and the data are compensated using the monthly average natural background noise level. The sampling rate is 10 seconds. The natural background noise level in the nighttime is usually 8–10 dB higher than the daytime level, owing to the effect of lightning noise from the southern tropical regions and the good propagation conditions of the night E-layer in the ionosphere. The average noise level of the north–south direction is always a few decibels higher than in the east–west direction because Ohshima Island is located south of the large man-made noise emission areas of Tokyo, Yokohama, and the large industrial area in Kanagawa prefecture.

Volcano microvibrations were observed at Ohshima observatory from July 1986 onward (Weather Record, 1987b), but the anomalous impulsive

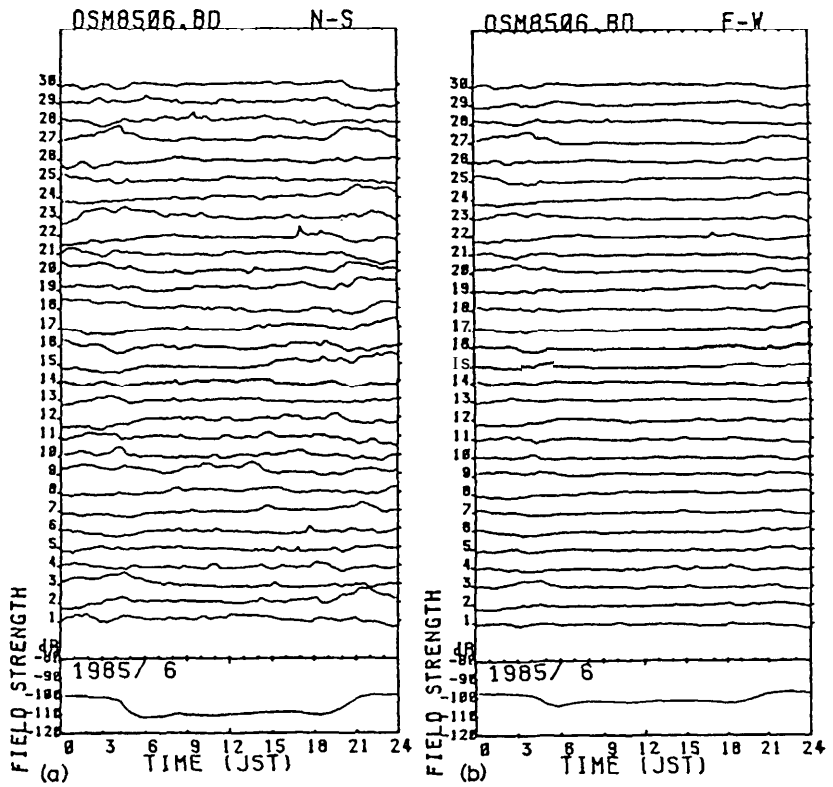

Fig. 14. Typical example of noise levels during the quiet period 17 months before the eruption. (a) North–south direction; (b) east–west direction. (After Yoshiro et al. 1989.)

noise emissions at 82 kHz did not appear until after October 20. The observation of several clear burst-like emissions were recorded from November 3–22. The plots of our improved analyzed data for a sampling time of 1 second at Ohshima on October 20 and during all of November are presented in Figure 15a, b, and c. Figure 15a shows the data for the first observed anomalous emission, Figure 15b shows the data from November 1–13, the

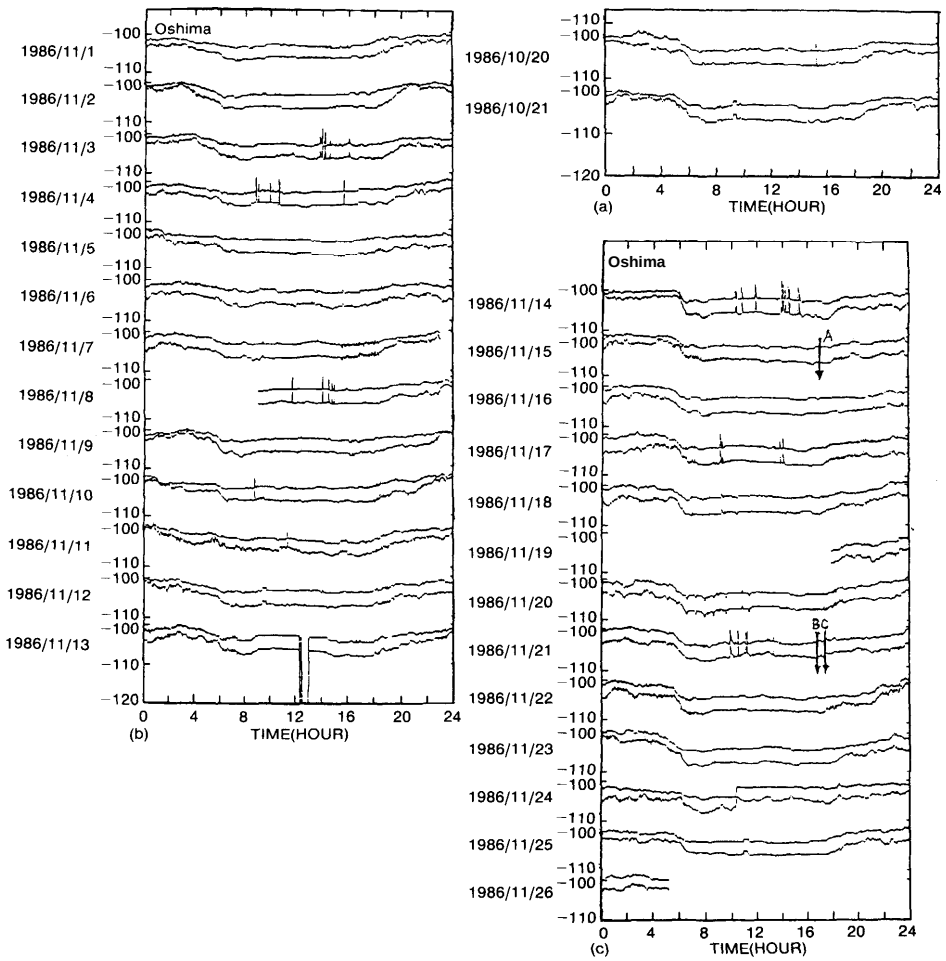

Fig. 15. (a) First clear anomalous burst-like emission of an 82-kHz magnetic field observed on October 20 at Ohshima, 26 days before the eruption. (b) Eighty-two kHz data for November 1–13 at Ohshima. The upper plots show the north–south directional data, and the lower plots show the east–west directional data. (c) Data for November 14–25 at Ohshima. The arrow on November 15 is the starting time of the eruption at summit crater A and the arrows on the 21st are the starting time of the eruptions in craters B and C. (After Yoshiro et al. 1989.)

two-week period just before the eruption, and Figure 15c shows the data for the eruption period from November 14–23. The upper plots show the noise level of the north–south sensor and the lower plots show the level or the east–west sensor. The noise level during the night is usually 6–10 dB higher than the daytime level as a result of lightning in the southern tropical region.

As shown in Figure 15a and b, the observation of burst-like emissions occurring four and two weeks prior to the first eruption were identified at 14–16 JST on November 3, at 09–11 and 16 JST on November 4, at 11:30 and 14–16 JST on November 8, at 09 JST on November 10, and at 11 JST on November 11.

At 17:25 JST on November 15, the first major eruption occurred in the main crater. The location of this crater is indicated as A in Figure 13. Anomalous burst-like emissions were observed at 10–16 JST on November 14, one day before this major eruption, but were not observed at the time of eruption. The volcanic activity continued with violent eruptions, and the lava fountain reached heights over 200 m. Lava flowed out from the summit crater A to the caldera at 10:35 JST on November 19, as shown in Figure 13. The earthquake and volcanic microvibrations during the eruption in crater A continued violently, and burst-like emissions were only observed at 08–09 JST and 14–15 JST on November 17, but the average background noise levels at night were 12–20 dB higher than the usual daytime levels. At 23 JST on November 19, the eruption activity of crater A quickly decreased.

At 10–12 JST on November 21, several strong burst-like emissions were observed, as shown in Figure 15c, the strongest peaks during these emissions reaching over 12 dB more than background noise level. At the same time, strong local earthquakes started and continued until evening. At 16:15 JST, 4 hours after the emissions at 10–12 JST, eruption occurred in 19 new craters, which appeared along a line trending NW–SE in the bottom of the old caldera. The location of this group of craters is labeled B, and shown in Figure 13.

At 16:15 JST, summit crater A (old crater) erupted violently, and at 17:45 JST new craters suddenly appeared in the virgin fields on the northwestern slope of the mountain. The location of this group of craters is labeled C in Figure 13. Lava flowed down rapidly toward the station at upper Motomachi, as shown in Figure 13. Motomachi has the largest population on this island. By special order from the Mayor of Tokyo, a state of emergency was declared and all of the 10,000 inhabitants of the island, except for a few scientists, policemen, and firefighters, were evacuated until the early morning of November 22. The major eruptions in crater B and C completely ceased on the morning of November 22. Our data recording also ceased after November 25 because the sensors were destroyed by the lava flow. Later on, our station was moved to a safer area near Nomashi village, 2 km south of Motomachi, and the replacement equipment continues to operate at Nomashi observatory.

Observed Results at an Eruption in Izu Itoh Bay in July 1989

Since early April 1989, volcanic microvibrations and earthquakes were observed at a very local area around the city of Izu-Itoh. After early June, the number and amplitude of these volcanic earthquakes increased significantly, and felt earthquakes increased to several hundred per day into early July. The inhabitants of the city were afraid and anxious to know the location of the next eruption, whether on the bottom of Ito Bay or on land. The worst case would be a sudden eruption in an area of high population density, with new craters erupting lava and scoria in the city. In this case, a huge number of lives would be lost, and be the major city of Itoh would be destroyed.

The observed magnetic field emissions increased in proportion to the increase in occurrence of volcanic earthquakes. Observations of magnetic field emissions at 1.525 kHz and 36 Hz at Ohshima Island increased during July 1–26 in 1989, as shown in Figure 16a and b. Many emissions were recorded from July 1 to noon of July 11, as shown in these figures, but after noon of July 11, the characteristics and levels of emissions seemed to change. The volcanic activity also changed. A very large number of volcanic earthquakes occurred before noon of July 11, but after this time, the volcanic activity changed suddenly from the volcanic earthquake mode to the strong volcanic vibration mode. Many inhabitants of Itoh city had listened to the loud sound incessantly like the striking of very large drums with many huge hammers, just under Itoh City. However, no clear emissions were observed during these violent volcanic vibrations after noon of July 11.

Fortunately, at 16:24 JST on July 13, the eruption started at a new crater in the bottom of Itoh Bay. This point was located only 2.5 km from the Itoh shore, on the eastern side of the Izu peninsula, as shown in Figure 17.

The key point in our observed data for this volcanic eruption is that we received very many emissions at 36 Hz during the time of active volcanic earthquakes, until approximately noon of July 11. Then, the mode of vibrations shifted from volcanic earthquakes to volcanic vibrations, and the emission signals ceased, as shown in Figure 16a and b. This result strongly suggests a most interesting point, namely that emission occurred when the rock was crushed in this event. Unfortunately, we could not obtain data in the most important time, from July 6–11, as mentioned above.

Discussion of the Source Mechanism

The observation of anomalous, burst-like emissions at 82 kHz does not directly correspond to the time of the initiation and duration of the most active eruptions, as can be deduced from inspection of Figures 4c, 7a, and 7b. In the case of Ohshima, the observed anomalous emissions at 10–12 JST on November 21 occurred 4–6 hours before the eruptions from the new craters on the virgin fields inside the caldera at point B and on the mountain slope outside the caldera at point *C*, as shown in Figure 13.

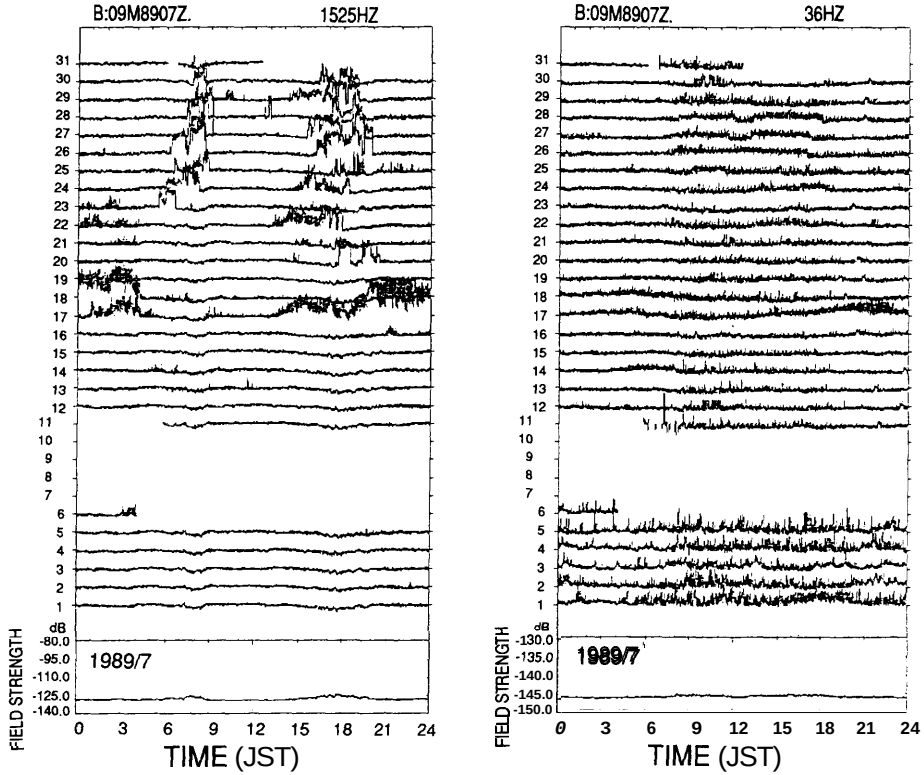

Fig. 16. Intensity of the seismogenic magnetic emissions observed at Izu-Ohshima in July 1989, during the volcanic activity and eruption at Izu Itoh Bay. 1.525 kHz, and (b) at 36 Hz, respectively. On 16:24 JST, July 13, 1989, a new crater erupted in the bottom of Ito Bay, and this point was located 2.5 km from the coast of a major city. Between July 6–11 there are no data owing to trouble with our marine telemetry cable, possibly an effect impending eruption.

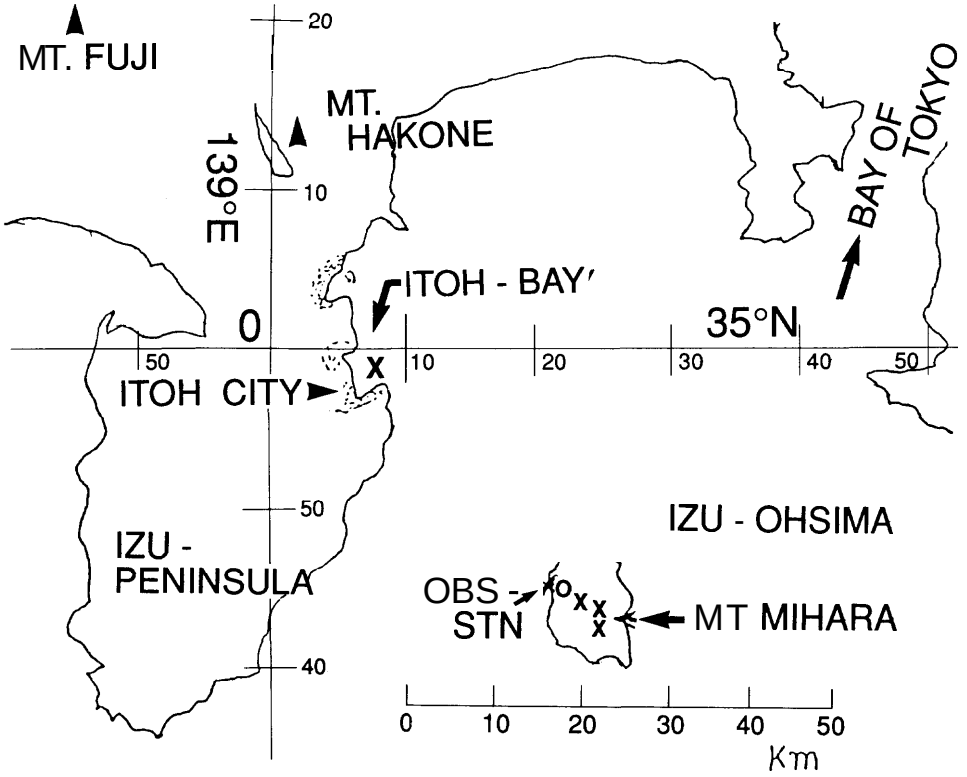

Fig. 17. Location of the new volcano which erupted in Izu Itoh Bay on July 13, 1989.

Geological studies after the eruption of Ohshima indicated that the mixing ratio of silica in the lava and scoria erupted from the summit crater A differed from that of the lava that extruded from locations B and C (Sasai, 1987; Utada, 1987; Weather Record, 1987c; Yoshino et al., 1989). These results suggest that the source of lava extruding from the summit crater A had a different source from the lava flow extruding at locations B and C. A preliminary model to explain the eruption mechanism of September 21 was developed by Prof. Aramaki of the Earthquake Research Laboratory, University of Tokyo. We have applied his model (Aramaki, 1987) to explain our observed results. Figure 18 shows the movement of magma based on this model. The mechanism for these anomalous burst-like emissions is explained as follows: (1) the magma flow to the eruption of the summit crater A was supplied directly from the base magma as primary magma Y; and (2) the eruptions in the new craters B and C were created by new magma flows, forced up as dikes inserted into the mountain body on the morning of November 21 (Aramaki, 1987).

The quantity of dike material seems to have been approximately equal to the size of magma volume for the total eruption of this volcano (Weather Record, 1987d). The basalt with a high mixture ratio of silica grains was formed under craters B and C by the heating effect of this dike, and this

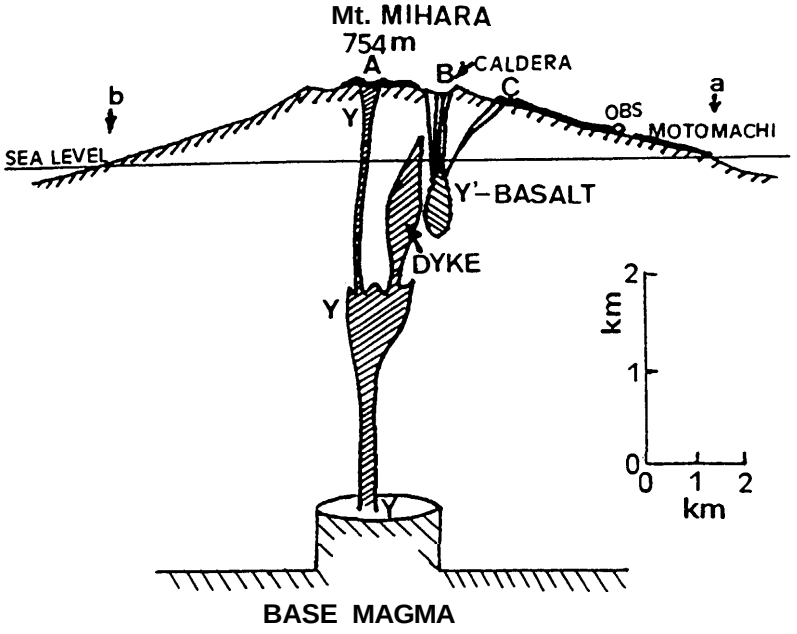

Fig. 18. Vertical profile of Mt. Mihara, illustrating the mechanism of magma flow in the mountain body based on the Aramaki (1987) model. The summit crater A erupted as a result of the insertion of the primary magma Y, and the new crater B and C, erupted as a result of basalt Y, which was heated by a dike of primary magma. The starting time of the dike insertion corresponds to the time of the burst-like emissions observed during 10–12 JST on November 21, 1986. (After Yoshiro et al. 1989.)

molten basalt was extruded 600 m from the mouth of the craters as a result of the high back pressure of the internal gas, which was created as a result of high density of silica grains. The eruption from craters B and C ceased a few hours after it began, and duration of this short but violent eruption fits the Aramaki model well. At the same time, data obtained from other kinds of instruments suggested that the commencement time on the dike insertion was around 10–12 JST on November 21 (Sasai, 1987; Yukutake et al., private communication, 1987).

To explain the emissions at dike insertion, we apply the results of laboratory experiments by Mizutani and Yamada (1987) and Cress et al. (1987). We believe that the observed emissions on November 21 were produced by the rock crushing due to the insertion of dikes. Emissions recorded during 10–16 JST on November 14, 10–14 JST on November 17, and the other various emissions that were observed before the eruptions from crater A, can be explained as the impulse emission induced during the intervals when cracks propagated through the rocks as a result of the movement of magma or dike intrusion prior to the eruption. These phenomena can be explained and the model developed can be proved by means of the results of the ongoing laboratory experiments of Cress and Mizutani.

Conclusion

As shown in this article, the building of a multipoint observation system for the prediction of earthquakes by use of the seismogenic electromagnetic emission phenomenon is progressing positively. The characteristics of the receiving system and the practical design of the details of facilities are completed, and now we are continuing the telemetry system development for high speed, high accuracy, the highest reliability, and the lowest operational cost for continuous and long-term automated operation. We are developing the computer software to obtain the most reliable detection algorithm for the prediction at the central computer, and also for transmission of data to the local earthquake alarm center.

The most important aspect for the development of this automatic alarm system is protection and discrimination against man-made noise interference. We are developing a noise-reduction method using a network spread over eight observation points, with a point-to-point distance of approximately 55 km. Each observation point consists of a LF (82 kHz) direction finding system. The bearing and signal intensities are converted to 16-bit digital values and transferred through a telemetry system to the computer in the warning center. When the cross-correlation appears to be high and the bearing data of all or several points are directed to one area, the alarm signal will transmit an earthquake warning and show the predicted epicenter area automatically. If the signal intensity is strong at only one or a few points and the calculated cross correlations are very low, this increase of signal intensity will be ignored as man-made noise interference. Although the author had only one case where we could clearly have predicted an epicenter location before an earthquake (Yoshiino et al., 1985), we continue to analyze other

observational data retrospectively. We believe strongly that this will be one of the most reliable systems for man-made noise reduction. And we have started the search for new observation frequencies in the VLF range, below the cut-off frequency of the VLF ionospheric guided-mode propagation (1.525 kHz) and the higher frequencies of ELF (36 Hz) in the Schumann resonance band. Attempts to eliminate natural noise interference from lightning discharges in tropical regions were started by our research groups.

In our investigations of the noise source and propagation path of seismogenic electromagnetic emissions as a precursor of earthquakes, we utilized the experimental results of electromagnetic emissions due to the crushing of rocks by Mizutani and Yamada (1987) and Cress et al. (1987) to explain the mechanism of emission around the focus of the earthquakes. We also applied the theory of surface mode propagation of electromagnetic waves along the boundary surface of a fault to explain why the energy transmission of seismogenic emission from the focus to the ground surface is less attenuated in comparison with the case of usual plane wave transmission. On the problem of the radiation mechanism of waves at the surface of the ground, the authors applied the radiation mechanism of slit antennas which consists of the top of the fault at the ground surface. However, the theoretical explanation of the impedance-matching between a surface mode transmission line and a slit antenna is very complicated, and still requires a more detailed investigation.

We roughly estimated the transmission loss by use of an optimum value, and averaged measurements for a typical fault in the Kanto area. We then concluded that the total attentuation loss for a specific case of the surface mode transmission and slit antenna radiation was 26 dB lower than the case of usual plane wave transmission without a fault. The precise investigations for this problem have to be continued for each earthquake observed from now on.

In this study, we presented the results of observed electromagnetic emissions related to the volcanic eruptions at Mt. Mihara on Izu-Ohshima Island during November, 1986, and at Izu Itoh Bay during July, 1989. These recordings are believed to represent the first observations of electromagnetic emissions during a volcanic eruption measured anywhere in the world. Since 1987, the data recorded at Ohshima have used one of the 82-kHz direction-finding detectors and two new frequencies at 1.525 kHz and 36 Hz in a multipoint receiving network around the Tokyo area which was designed for the detection of electromagnetic emissions prior to earthquakes. This earthquake prediction experiment was started in 1982.

A large number of data sets were obtained by other kinds of instruments during the time interval mentioned above, including: DC, ELF, and VLF conductivity, telluric currents, total magnetic-flux density, gravity, seismology, volcanic microvibrations, etc. (Sasai, 1987; Utada, 1987; Weather Record, 1987d; Yoshino & Tomizawa, 1989; Yukutake, private communication, 1987). These data support the theory that dikes branched off from the primary magma intrusion in the case of Mt. Mihara, as shown in Figure 18.

These observations suggest that the source mechanism of emissions at Mt. Mihara can be explained by the Aramaki (1987) model, as well as the more interesting observational results obtained from the volcanic eruption in the Izu Itoh Bay on July 13, 1989, and the experimental results of the ongoing laboratory experiments by Cress et al. (1987) and Mizutani and Yamada (1987).

Author's note. A portion of this research was financially supported by Japan IBM Corporation in 1986.

References

Aramaki, S. (1987). A suggestion of possibilities of dike insertion at the eruption on November 21, 1985. *Symposium on the Eruption of the Izu-Ohshimu Volcano in* 1986. Tokyo University, 11–15, April (extended abstract).

Cress, G. O., Brady, B. T., & Rowell, G. A. (1987). Source of electromagnetic radiation from fracture of rock samples in the laboratory. *Geophysics Research Letters, 14,* 331–334.

Cullen, A. L. (1954). The excitation of plane surface waves. *IEE Part IV,* 101, 225.

Chmyrev, V. M. et al. (1987). Electric fields and hydromagnetic waves in the ionosphere over the earthquake centre. *IUGG Abstracts,* 1, 384.

Gokhberg, M. B. (1984). The models of electromagnetic processes related to seismotectonics. *Terra Cognita, 4,* 369.

Gokhberg, M. B. et al. (1987). The earthquake preparation processes and earth's crust electromagnetic emission connecting modeling. *IUGG Abstracts,* 1, 382.

Gokhberg, M. B., Morgounov, V. A., Yoshino, T., & Tomizawa, I. (1982). Experimental measurement of electromagnetic emissions possibly related to earthquakes in Japan. *Journal of Geophysics Research.* 87. 7824–7827.

Goubou, G. (1950). Surface waves and their application to transmission lines. *Journal of Applied Physics, 21,* 1119.

Larkina, V. I. et al. (1987). Low frequency emission data in upper ionosphere over the earthquake center. *IUGG Abstracts, 1,* 384.

Migulin, V. V. et al. (1987). Earthquake electromagnetic forerunner diagnostic problems by wave experiment low latitude satellite data. *IUGG Abstracts, 1,* 384.

Mizutani, H., & Yamada, I. (1987). Electromagnetic emission and acoustic emission associated with rock deformation. XIX General Assembly of the IUGG, Vancouver. *Abstracts,* 1, 384.

Sasai, Y. (1987). Geomagnetic field variations before and after the eruption of the Izu-Ohshima volcano in 1986. Tokyo University 23–25, April (extended abstract).

Utada, H. (1987). Variations in the electrical resistance before and after the eruption of the Izu-Ohshima volcano in 1986. Tokyo University, 26–28, April (extended abstract).

Weather Record (Japanese Meteorological Agency—JMA), Volcano Research Section of JMA (1987a). Special Issue on the eruption of the Izu-Ohshima volcano in 1986. *Kisho, 31*(1), 8–25 (in Japanese).

Weather Record (1987b). *Kisho, 31*(1), 35–44.

Weather Record (1987c). *Kisho, 31*(1), 26–33.

Weather Record (1987d). *Kisho,* 31(1), 74–82.

Yoshino, T. (1986a). On the study of electromagnetic emissions related to earthquakes and application to earthquake prediction, *JIEICE Technical Report, 85,* 19–24, 313 (in Japanese).

Yoshino, T. (1986b). The EM emission phenomena as a precursor of earthquakes and the possibility of epicenter location prediction. *Proceedings of the 8th International Wroclaw Symposium EMC, 8,* 5–14.

Yoshino, T., & Tomizawa, I. (1989). Observation results of low-frequency electromagnetic emissions as precursors of the volcano eruption at Mt. Mihara during November 1986. *Physics of the Earth and Planetary Interiors,* 57, 32–39.

Yoshino, T., Tomizawa, I., & Shibata, T. (1985). The possibility of using a direction finding technique to locate earthquake epicenters from electromagnetic precursor radiation. *Annales Geophysicae,* **3,** 727–730.